Amino Acids (2018) 50:309–320
https://doi.org/10.1007/s00726-017-2517-z

ORIGINAL ARTICLE

Imaging the expression of glypican-3 in hepatocellular carcinoma by PET

Zhen Wang[1,2] · Yan-Jiang Han[1] · Shun Huang[1] · Meng Wang[1] · Wen-Lan Zhou[1] · Hong-Sheng Li[1] · Quan-Shi Wang[1] · Hu-Bing Wu[1]

Received: 10 June 2017 / Accepted: 21 November 2017 / Published online: 4 December 2017

Abstract

The glypican-3 (GPC3) receptor is overexpressed in hepatocellular carcinoma (HCC) and is a potential diagnostic and therapeutic target. GPC3-targeted molecular imaging will be helpful to differentiate diagnosis and guide therapy. In the present study, we will develop a novel PET probe for imaging the expression of GPC-3. L5 (sequence: RLNVGGTYFLTTRQ), a GPC3 targeting peptide, was labeled with 5-carboxyfluorescein (FAM) and ^{18}F-fluoride. Cell binding tests were performed to identify the binding specificity of FAM-L5 and ^{18}F radiolabeled peptide. MicroPET/CT imaging was used to determine the potential of a novel PET tracer for visualizing HCC tumors with a high expression of GPC3. In vitro binding tests showed that the uptake of FAM-L5 in HepG2 cells (high expression of GPC3) was significantly higher than that of HL-7702 cells (negative expression of GPC3) (mean fluorescent intensity: 14,094 ± 797 vs. 2765 ± 314 events, $t = 32.363$, $P = 0.000$). Confocal fluorescent imaging identified that FAM-L5 accumulated where the GPC3 receptor was located. A novel PET tracer (^{18}F-AlF-NODA-MP-6-Aoc-L5) was successfully labeled by chelation chemistry. In vitro cell uptake studies showed that ^{18}F-AlF-NODA-MP-6-Aoc-L5 can bind to HepG2 tumor cells and was stable in PBS and mouse serum stability tests. MicroPET/CT showed that HepG2 tumors could be clearly visualized with a tumor/muscle ratio of 2.46 ± 0.53. However, the tumor/liver ratio was low (0.93 ± 0.16) due to the high physiological uptake in the liver. This study demonstrates that FAM and the ^{18}F-labeled L5 peptide can selectively target HCC with a high expression of GPC3 in vitro and in vivo. ^{18}F-AlF-NODA-MP-C6-L5 has the potential to be a GPC3 target tracer but requires some chemical modifications to achieve a high enough tumor/liver ratio for detection of the tumor in the liver.

Keywords Hepatocellular carcinoma · Glypican-3 · Targeting peptide probe · Fluorescent imaging · PET

Abbreviations

GPC3	Glypican-3
HCC	Hepatocellular carcinoma
FAM	5-Carboxyfluorescein
TACE	Transarterial radioembolization
PET	Positron emission tomography
HPLC	High-performance liquid chromatography
DAPI	4,6-Diamidino-2-phenylindole
DMEM	Dulbecco's modified Eagle's medium
PBS	Phosphate-buffered saline
OSEM	Ordered subsets expectation maximum
IRW	Inveon Research Workplace
ROI	Region of interest
VOI	Volume of interest

Handling Editor: G. J. Peters.

✉ Quan-Shi Wang
wqslph@163.net

✉ Hu-Bing Wu
wuhbym@tom.com

[1] Nanfang PET Center, Nanfang Hospital, Southern Medical University, 1838 Guangzhou Avenue North, Guangzhou 510515, Guangdong, China

[2] PET Center, The First Affiliated Hospital, College of Medicine, Zhejiang University, Hangzhou, Zhejiang, China

Introduction

Hepatocellular carcinoma (HCC), which accounts for 75% of liver cancer cases, is currently the third leading cause of cancer-related deaths globally, causing approximately 782,000 annual deaths (Torre et al. 2015; Mittal and El-Serag 2013; Forner et al. 2012). The incidence of HCC has

been increasing in the past decade largely in parallel to the incidence and duration of exposure to Hepatitis B and C (Chan et al. 2004; Tseng et al. 2012). For early stage HCC, liver resection, percutaneous ablation,radiologic intervention and transplantation are always recommended for treatment (Bruix and Sherman 2011; Bruix et al. 2016; Akoad and Pomfret 2015; Chen et al. 2016; Shiina et al. 2012). However, most patients who are diagnosed with HCC are ineligible for curative local therapy. Management of advanced HCC has presented a therapeutic challenge. Transarterial radioembolization (TACE) combined with systemic chemotherapy treatment were commonly used, but the outcomes in disease control were disappointing (Bertino et al. 2013; Paul et al. 2009; Samonakis and Kouroumalis 2017; Moriguchi et al. 2016). Molecular-targeted treatments are a new modality that has emerged as a potential treatment for advanced HCC (Chuma et al. 2015; Chan et al. 2015).

Glypican-3 (GPC3) is a membrane-associated heparan sulfate proteoglycan that was reported to be over-expressed in up to 50–80% of human HCCs, while its expression is absent in normal adult tissues (Suzuki et al. 2010; Yan et al. 2011; Liu et al. 2010, 2015; Coston et al. 2008; Enan et al. 2013; Libbrecht et al. 2006; Ho and Kim 2011; Chen et al. 2014). By stimulating the canonical Wnt signaling pathway, GPC3 creates a significant effect in mediating the hepatocyte malignant transformation and promoting HCC growth, and it plays a crucial role in HCC metastasis (Gao et al. 2014; Lai et al. 2010). Therefore, it now appears to be a potential imaging and therapeutic target for HCC (Yao et al. 2014; Qi et al. 2014; Hanaoka et al. 2015; Feng et al. 2013; Sawada et al. 2016).

Therefore, because GPC3 is not over-expressed on each HCC, patient selection is very important for GPC3-targeted treatment. A GPC3 targeting molecular imaging technique may give us the capacity to noninvasively study GPC3 expression in vivo, which will play an important role in guiding treatment, as well as in characterizing HCC. Positron emission tomography (PET) imaging with a ^{89}Zr-conjugated monoclonal antibody(mAbs) or F(ab′)$_2$ fragment directed against GPC3 has been successfully established and has shown promise (Sham et al. 2014a, b; Yang et al. 2014). However, ^{89}Zr is not available in some countries, such as China, and needs to be imported from other countries, which makes it inconvenient in clinical practice. As an alternative, peptide-based PET probes, especially those radiolabeled with ^{18}F, are easier to transfer into the clinic because ^{18}F can be easily obtained in those PET centers with cyclotron (Wu et al. 2007; Schottelius and Wester 2009). Unfortunately, as far as we know, no PET peptide tracer has been introduced yet.

A GPC3 targeting peptide (named L5) was previously identified by Lee et al. (2011) using proteomic mass spectrometry. In the present study, we attempted to develop a novel PET tracer of ^{18}F-AlF-NOTA-MP-6-Aoc-L5 (NODA: 1,4,7-triazacyclononane-1,4-diacetate; MP: methylbenzyl; 6-Aoc: 6-aminocaproic, as a spacer) by radiolabeling the L5 peptide with a positron emitter of ^{18}F. It was reported that Aoc, as a spacer, is helpful for efficiently clearing radioactivity from the blood pool by excretion mainly through the renal/urinary pathway (Prasanphanich et al. 2007, 2009), but not via the hepatobiliary system, which may be useful for imaging HCC tumors. Additionally, to confirm its targetability, we also labeled L5 with FAM fluorescence (5-carboxyfluorescein) to observe the uptake of this fluorescent probe in cells in vitro.

Materials and methods

Materials

All the commercially available chemicals were used as purchased. The L5 peptide containing 14 amino acid residues (sequence: RLNVGGTYFLTTRQ) (Lee et al. 2011) and the FAM-labeled L5 (FAM-L5) were custom manufactured by China Peptides Co., Ltd. (Shanghai, China). NODA-MP-C6-L5 was custom manufactured by the Chinese Peptides company (Shanghai, China). Rabbit anti-GPC3 antibody was purchased from Abcam Ltd. (Shanghai, China). Dylight 647-conjugator Cy3-conjugated secondary antibody and 4,6-diamidino-2-phenylindole (DAPI) were purchased from Beyotime (Shanghai, China). No-carrier-added ^{18}F-F was obtained from an in-house PETtrace cyclotron (GE Healthcare, America). Reverse-phase extraction C18 Sep-Pak cartridges, syringe filters and polyethersulfone membranes (pore size 0.22 μm; diameter 13 mm) were obtained from Waters (Massachusetts, USA) and were pretreated with anhydrous ethanol and deionized water immediately prior to use. The cold, radiolabeled peptides were identified using an analytical high-performance liquidchromatography (HPLC) system (Shimadzu, Japan) consisting of an LC-10AD pump, a variable wavelength SPD-M20A UV detector and a Flow-Count radio-HPLC Detector (Bioscan). The reverse-HPLC solvents were 0.1% CF_3COOH in H_2O (solvent A) and 0.1% CF_3COOH in acetonitrile (solvent B). The flow rate was 1 ml/min with the mobile phase starting from 95% solvent A (0.1% TFA in water) to 20% solvent A and 80% solvent B for 25.0 min. The UV absorbance was monitored at 214 and 254 nm. The LC column that was used was a ZORBAX Eclipse XDB-C18 4.6 × 150 mm, 5 μm.

Tumor cell lines

A human HCC cell line, HepG2, with over-expressed GPC3 and the human liver cell line HL-7702, which negatively expresses GPC3, were purchased from the Institute

of Biochemistry and Cell Biology, Shanghai Institutes for Biological Sciences, Chinese Academy of Sciences (Shanghai, China). Cells were cultured in Dulbecco's modified Eagle's medium (DMEM) (HyClone, Logan, USA) supplemented with 10% fetal bovine serum (HyClone, Logan, USA) at 37 °C in a humidified 5% carbon dioxide-containing atmosphere.

GPC3 expression and cell binding of FAM-L5 in vitro

GPC3 expression was determined by an indirect immunofluorescence assay. HepG2 and HL-7702 cells were plated onto six-chamber slides and incubated at 37 °C overnight with primary anti-GPC3 antibody diluted 100 times (1 μg/mL) after fixing with 4% paraformaldehyde solution. They were then washed with phosphate-buffered saline (PBS) solution and incubated with Cys3-conjugated second antibody for 1 h. After staining with 4′, 6-diamidino-2-phenylindole (DAPI) for nuclear counter staining, GPC3 expression was visualized under a fluorescent inversion microscope.

The binding ability of FAM-L5 to cells positively expressing GPC 3 in vitro was assessed via fluorescence microscopy and flow cytometry. 1×10^5 HepG2 cells were incubated with 10 μM of FAM-L5 in PBS/1% BSA at 37 °C for 1 h. After that, the cells that were bound by FAM-L5 were imaged using a fluorescent inversion microscope (Olympus IX71). HL-7702 cells incubated with 10 μM of FAM-L5 were selected as a control. When imaging using the fluorescent microscope, white light was used to confirm that tumor cells were in the field of view. Then, in the same field of view, blue light was used to visualize the green light emitted from the cells and to take the photos. The uptake intensity of FAM-L5 on the cells was quantified by using BD LSRFortessa flow cytometry (BD Biosciences, New Jersey, USA). The fluorescence excitation wavelength was 488 nm and the emission was measured with a filter of 578 nm using the blue Laser.

Synthesis of PET molecular probe, ^{18}F-AlF-NODA-MP-6-Aoc-L5

The radiolabeling of NODA-MP-6-Aoc-L5 peptides was performed according to a previously published procedure (Chatalic et al. 2014; Dijkgraaf et al. 2012; McBride et al. 2009). Briefly, 5 μl of glacial acetic acid and 340 μL of acetonitrile (nearly 70% v/v) were added with 250 μg (11.7 μmol) of NODA-MP-6-Aoc-L5 peptide in 100 μl DI of water to a 2-ml plastic tube containing 6 μl of 2-mM aluminum chloride (1.6 ug, 1.2 nM). After a brief vibration, the mixture was added with 50 μL ^{18}F-fluoride (1.110–1.850 GBq). The pH of mixture was determined to be approximately 4.2. The tube was sealed and heated at 100 °C for 10 min. After that, the tube was cooled to room temperature, and the reaction mixture diluted with 15 mL of water along with the desired product were trapped on a Varian Bond Elut C18 column (100 mg) using a 15-ml syringe. The column was washed with another 10 mL of PBS and 20 mL of water, and the radioactivity trapped on the C18 column was eluted with 0.4 mL of ethanol containing 10 mM of HCl. The ethanol solution was diluted with PBS for further study. The formulated saline mixture was sterile-filtered into a sterile product vial. The purifies of NODA-MP-6-Aoc-L5 or corresponding radiolabelled peptide were determined on HPLC.

Partition coefficient

The partition coefficient value was expressed as log P. Log P of ^{18}F-AlF-NODA-MP-6-Aoc-L5 was determined by measuring the distribution of the radioactivity in 1-octanol and PBS. Approximately 370 kBq of ^{18}F-AlF-NODA-MP-6-Aoc-L5 in 2 μL of PBS (pH 7.4) was added to a vial containing 0.5 ml of 1-octanol and 0.5 mL of PBS (pH 7.4). After vigorously vortexing for 10 min, the vial was centrifuged at 12,500 rpm for 5 min to ensure complete separation of the layers. One hundred μL of each layer was pipetted into the test tubes, and the radioactivity was measured using a gamma counter (GC-1200, USTC Chuangxin Co. Ltd. Zonkia Branch, China). The mean value was calculated from the triplicate experiments.

In vitro stability determination

The stability of ^{18}F-AlF-NODA-MP-6-Aoc-L5 was tested in PBS and mouse serum. In brief, 3.7 MBq of ^{18}F-AlF-NODA-MP-6-Aoc-L5 was pipetted into 0.5 mL of the PBS or mouse serum and incubated in PBS at room temperature or mouse serum at 37 °C with gentle shaking at 300 rpm. The stability test was only performed at 2 h due to the short half life time of ^{18}F. To study PBS, an aliquot of solution was directly taken and the radiochemical purity was determined by reverse-phase HPLC under identical conditions at 2 h. For the mouse serum study, trifluoroacetic acid was added, and the soluble fraction was clarified with a 0.22-mm filter at 2 h. An aliquot of solution was then taken, and the radiochemical purity was determined by reverse-phase HPLC under identical conditions.

Cell binding assay of ^{18}F-AlF-NODA-MP-6-Aoc-L5 and blocking test

HepG2 cells (1×10^6 cells/plate) were plated at a uniform cell density and incubated overnight. The cells were washed twice for 2 min with ice-cold binding buffer (DMEM and 1% BSA). The cells were then incubated for 15, 30, 60, 90, 120 min at 37 °C with 185 kBq of

^{18}F-AlF-NODA-MP-6-Aoc-L5. To assess whether ^{18}F-AlF-NODA-MP-6-Aoc-L5 binding could be blocked by unlabeled L5, HepG2 cells were incubated with 185 kBq of ^{18}F-AlF-NODA-MP-6-Aoc-L5 and cold L5 (0.35 mmol/L) for 15, 30, 60, 90, 120 min at 37 °C. After washing with ice-cold binding buffer three times, the cells were lysed in 200 µL of 1-M NaOH. The cell-associated radioactivity was then measured using a gamma counter (GC-1200, USTC Chuangxin Co. Ltd. Zonkia Branch, China). Experiments were conducted in triplicate.

Animal model

Animal experiments were conducted under a protocol approved by the Nanfang Hospital Animal Ethics Committee at the Southern Medical University (Application No: NFYY-2013-159).

Male and female BALB/C athymic nude mice aged 4–6 weeks of age were obtained from the Laboratory Animal Center at Southern Medical University. HepG2 cells (HCC) were inoculated into the mice by injecting 1×10^6 cells subcutaneously into the left flank. Tumor xenografts were monitored until the largest tumor diameter was approximately 0.5–1 cm, which took 3–5 weeks.

MicroPET/CT imaging and blocking experiment

A microPET/CT scan was performed on a SIEMENS Inveon scanner (Siemens, Germany). HepG2 tumor-bearing mice ($n = 5$) were intravenously injected with 3.7–7.4 MBq (100–200 µCi) of ^{18}F-AlF-NODA-MP-6-Aoc-L5. MicroPET/CT images were acquired as 10-min static images 60 min after the injection with the mice under isoflurane anesthesia. For the blocking experiment, mice bearing HepG2 tumors were scanned (10-min static) at 1 h after coinjection of 3.7–7.4 MBq of ^{18}F-AlF-NODA-MP-6-Aoc-L5 with 20 mg/kg L5 peptide per mouse. The images were reconstructed by a 3-dimensional ordered subset expectation maximization (OSEM) algorithm, and CT was applied for attenuation correction.

In the PET images, the ROIs were measured with Inveon Research Workplace (IRW) 3.0 software (Siemens, Germany). The ROI was determined by manually superimposing the ellipsoid volume of interest (VOI) on the target tissue. The activity concentrations were determined by the mean pixel intensity within each VOI and converted to µCi/mL using a calibration constant. Assuming the tissue density of 1 g/mL, the ROI activity was converted to µCi/g and normalized as the percent injected dose per gram (%ID/g). The tumor/normal liver ratios and tumour/normal muscle were calculated by dividing the ROI activity in the tumor by that in the normal liver and muscle (Guo et al. 2012).

Statistical analysis

Descriptive data were expressed as the mean ± standard deviation. The Statistical Package for the Social Sciences, version 16.0 (SPSS Inc.), was used for statistical analysis. The nonparametric one-sample Kolmogorov–Smirnov test was applied to assess for normality. A p value greater than 0.05 indicated that the data were normally distributed. An independent sample t test was used to compare the two independent samples. A p value less than 0.05 was considered statistically significant.

Results

Chemistry and binding affinity

ESI-HRMS of the custom peptides was provided by China Peptides Co., Ltd. (Shanghai, China) for L5 and FAM-L5 and by the Chinese Peptides Company for NODA-MP-6-Aoc-L5. The calculated molecular weights were 1625.86 for L5, 1984.18 for FAM-L5 and 2131.0 for NODA-MP-6-Aoc-L5. The ESI-HRMS m/z [M + H] was found to be 1626.1 for L5, 1985.0 for FAM-L5 and 2130.0 for NODA-MP-6-Aoc-L5 (Fig. 1). The purities of the L5 peptide (99.15%), FAM-L5 (98.44%) and NODA-MP-6-Aoc-L5 (96.21%) were determined by analytical HPLC.

The dissociation constant (K_d) of L5 and NODA-MP-6-Aoc-L5 for binding with GPC3 were determined using surface plasmon resonance (SPR) measurements and were 4.47×10^{-8} and 1.01×10^{-7} mol, respectively, which revealed that the affinity of NODA-MP-6-Aoc-L5 was lower than that of intact L5.

Expression of GPC-3 receptors and in vitro cell uptake of FMA-L5

Immunofluorescence imaging was used to confirm the receptor expression. Strong fluorescence was detected in HepG2 cells. In contrast, only weak fluorescence could be seen in HL-7704 cells, indicating the positive expression of GPC-3 receptors on HepG2 cells, but the negative expression on HL-7704 cells (Fig. 2A1–A3, B1–B3). When FAM-L5 was incubated with HepG2 cells and HL-7704 cells at a concentration of 10 µM, FAM-L5 was found to be strongly taken up by the HepG2 cells (Fig. 1C1, C2) but not by the HL-7704 cells (Fig. 2D1, D2). The flow cytometry examination demonstrated the significantly higher uptake of FAM-L5 on HepG2 cells, compared to that of HL-7704 cells (14,094 ± 797 vs. 2765 ± 314 events, $t = 32.363$, $P = 0.000$) (Fig. 2E), indicating the specific binding of FAM-L5 to the GPC3 receptor. Confocal fluorescent imaging with a high-power lens further identified that FAM-L5 accumulated at

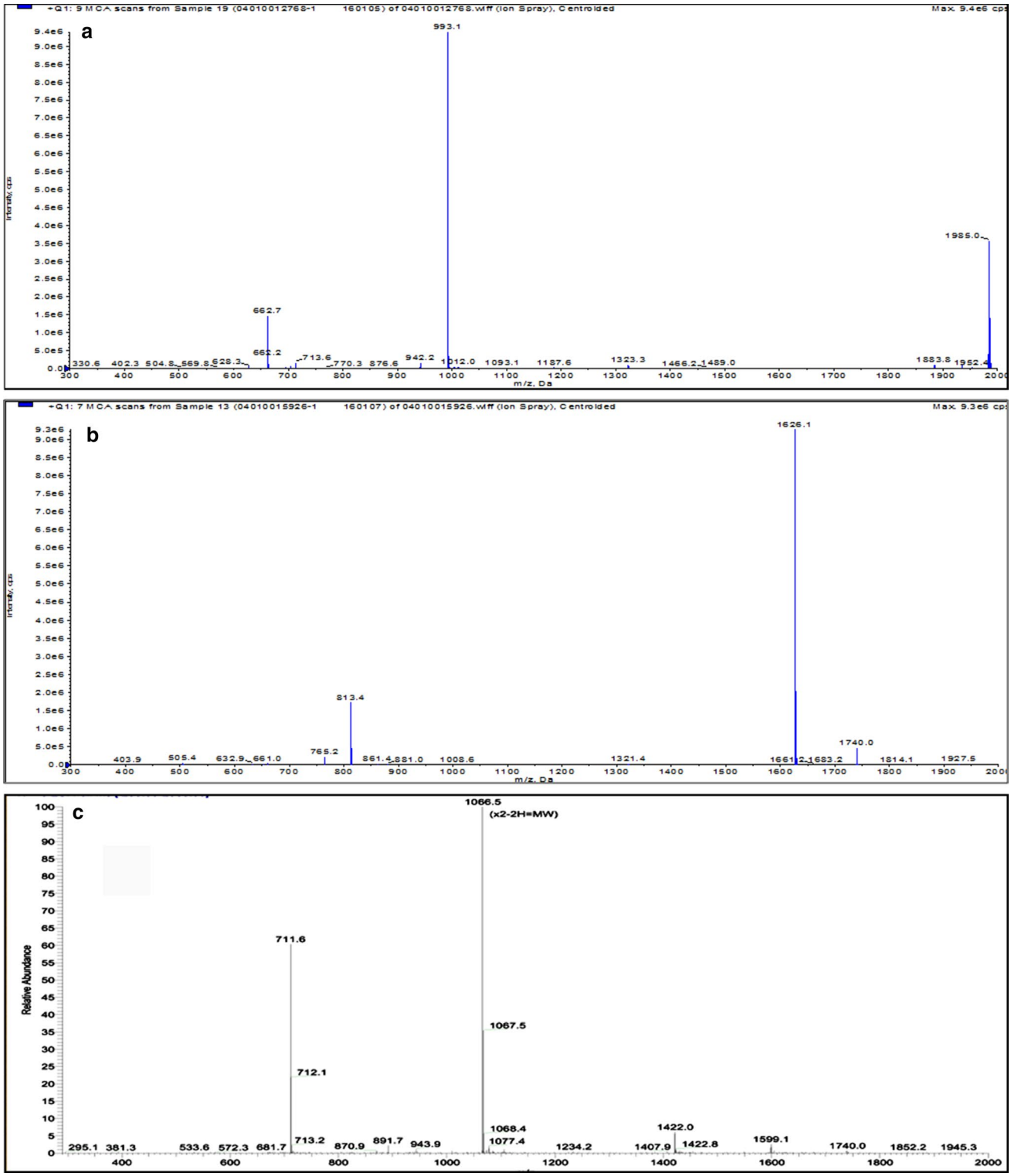

Fig. 1 ESI-HRMS of custom peptides. **a** ESI-HRMS *m/z* [M + H] was: 1626.1 for L5. **b** 1985.0 for FAM-L5. **c** 2130.0 for NODA-MP-6-Aoc-L5

the site of the GPC3 receptor, which was verified by overlapping the corresponding individual pictures (Fig. 3). FAM-L5 was not internalized into the cells because no obvious fluorescence was found in the cytoplasm.

Radiolabeling, log *P* value and in vitro stability of ^{18}F-AlF-NODA-MP-6-Aoc-L5

^{18}F-AlF-NODA-MP-6-Aoc-L5 was labeled by chelation

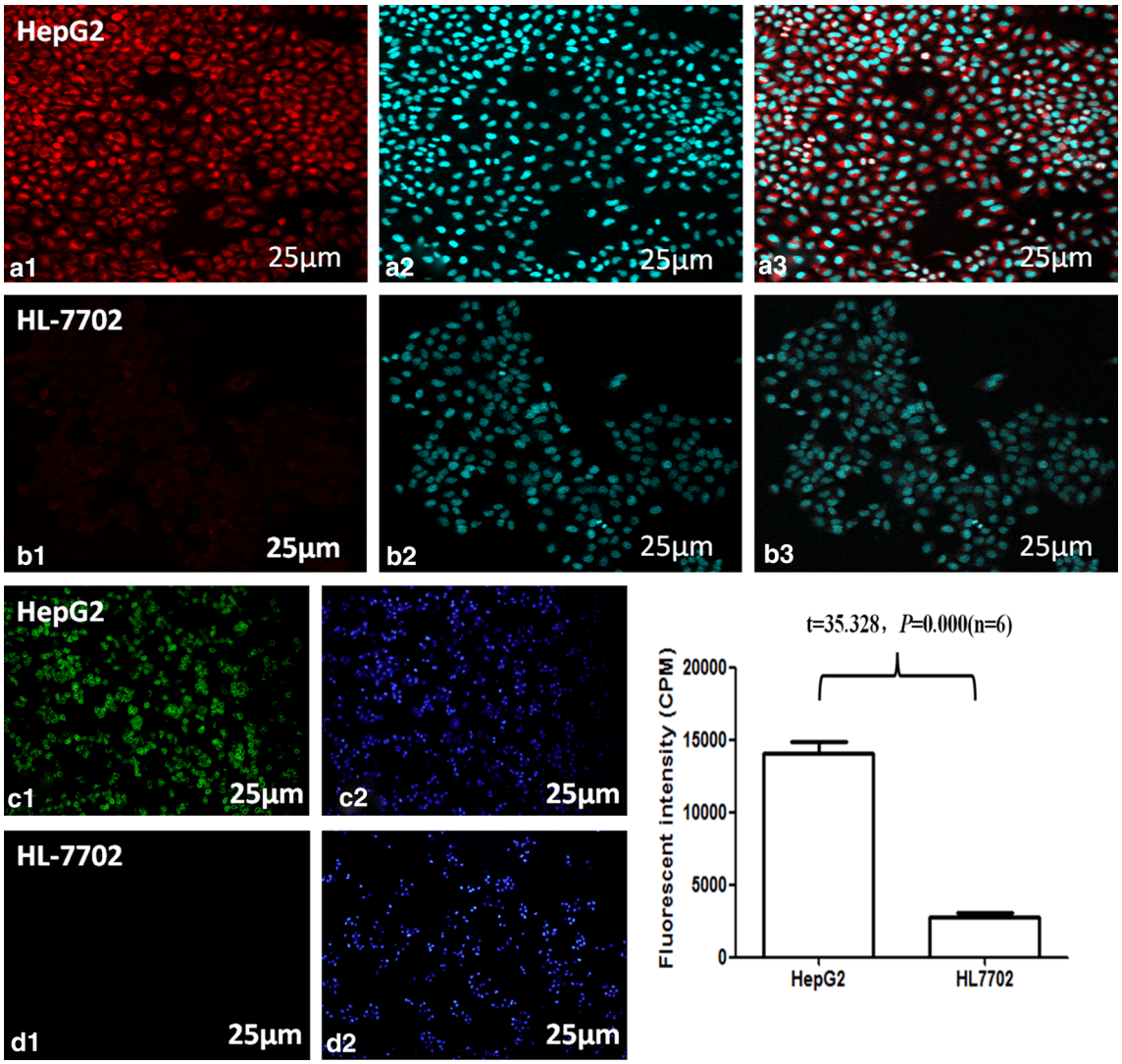

Fig. 2 GPC3 expression and FAM-L5 uptake on HepG2 and HL-7702 cells. A1–A3, B1–B3 Positive expression of GPC3 was detected in HepG2 cells but was negative in HL-7702 cells. A1, B1 GPC 3 expression (red). A2, B2 Nuclei were stained with DAPI (blue). A3, B3 Fused images of A1 with A2 and B1 with B2) (original magnification ×40; scale bars 25 μm). C1, C2, D1, D2 FAM-L5 was strongly taken up by HCC cells but not by HL-7702 cells after incubation for 1 h. C1, D1 FAM-L5 uptake (green). C2, D2 Nuclei were stained with DAPI (blue) (original magnification ×40; scale bars 25 μm). **E** Quantification of fluorescence revealed that the average level of FAM-L5 in HepG2 cells was significantly higher than that in the HL-7702 cells ($P = 0.000$)

chemistry. The radiochemical yield (without decay correction) was 20–56% (36.6 ± 14.0%). NODA-MP-6-Aoc-L5 and ^{18}F-AlF-NODA-MP-6-Aoc-L5 were analyzed by HPLC. The HPLC retention times of NODA-MP-6-Aoc-L5 and ^{18}F-AlF-NODA-MP-6-Aoc-L5 were 14.2 min and 14.7 min (Fig. 4), respectively, under the analytical condition. The radiochemical purity of the labeled peptides was greater than 95% (Fig. 4). The maximum specific activity of ^{18}F-AlF-NODA-MP-6-Aoc-L5 was approximately 37×10^3 Bq/mol.

The octanol/water partition coefficient (log *P*) for ^{18}F-AlF-NODA-MP-6-Aoc-L5 was determined to be − 2.88 ± 0.13, suggesting that radiolabeled peptide is rather hydrophilic. Based on the HPLC analysis, the in vitro stability was high. After 2 h of incubation, 95.9% and more than 98% of the ^{18}F-AlF-NODA-MP-6-Aoc-L5 peptide remained intact in the PBS and mouse serum, respectively.

In vitro cell uptake of ^{18}F-AlF-NODA-MP-6-Aoc-L5

Cell uptake of ^{18}F-AlF-NODA-MP-6-Aoc-L5 was examined in HepG2 tumor cells. The cell uptake study demonstrated that ^{18}F-AlF-NODA-MP-6-Aoc-L5 bound to HepG2 tumor cells. At 15 min of incubation, the cell uptake was approximately 1.0% of the ^{18}F-AlF-NODA-MP-6-Aoc-L5 and then reached approximately 2.0% at 60 min. After that, the cell uptake slightly increased to approximately 2.5% at 120 min

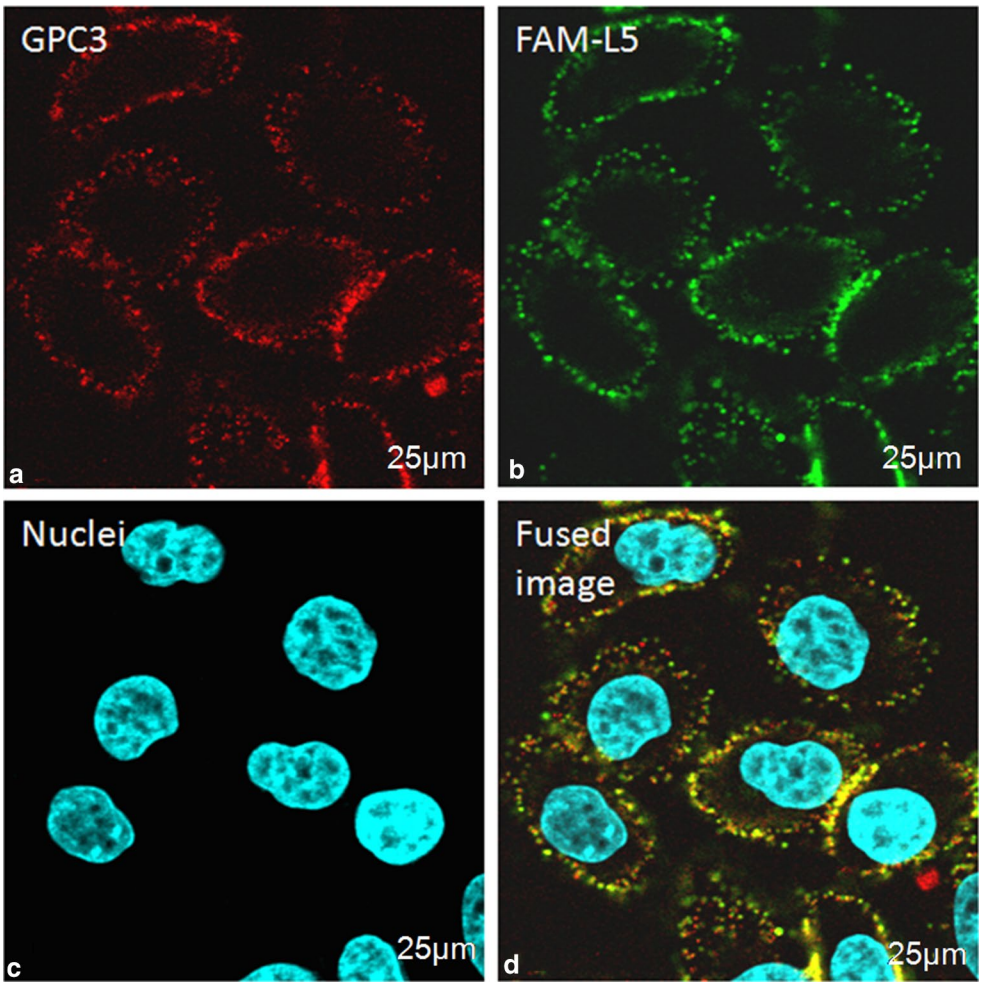

Fig. 3 The location of the GPC3 expression and FAM-L5 binding on the HepG2 cells. **a** GPC3 (red) was highly expressed on the membrane of the cells. **b** FAM-L5 (green) was strongly taken up by cells after 1 h of incubation. **c** Nuclei were stained with DAPI (blue). **d** Co-localization of FAM-L5 and GPC3. FAM-L5 was taken up at the same location as the GPC3 receptor (original magnification ×40; scale bars 25 μm)

(Fig. 5). Blocked with excess cold peptide, the cell uptake was kept at a relatively low level of < 1.0% of the input radioactivity (Fig. 5).

^{18}F-AlF-NODA-MP-6-Aoc-L5 micro-PET/CT for visualizing the HepG2 tumor in vivo

The maximum-intensity images (MIP) of the in vivo microPET/CT imaging in the subcutaneous HepG2 xenograft model at 60 min after ^{18}F-AlF-NODA-MP-6-Aoc-L5 injection is presented in Fig. 6a. HepG2 tumors were clearly visualized with a radioactivity uptake of 2.78 ± 0.42%ID/g (Figs. 6a, 7a). Minimal radioactivity was found in the brain, head and neck, lungs, heart, muscle and bones; however, the uptake of ^{18}F-AlF-NODA-MP-6-Aoc-L5 in the liver, gallbladder, intestine, kidneys and bladder was high (Figs. 6a, 7a), which contributed to a high tumor/muscle ratio (2.46 ± 0.53), but a low tumor/liver ratio (0.93 ± 0.16) (Fig. 7b). Low radioactivity distribution in the bones implied that the defluorination of ^{18}F-AlF-NODA-MP-6-Aoc-L5 did not occur in vivo.

Blocking tests were performed by intravenously treating with ^{18}F-AlF-NODA-MP-C6-L5 and excess amount of non-conjugated L5 peptide. The uptake of ^{18}F-AlF-NODA-MP-6-Aoc-L5 was found to be minimal in the tumor, leading to the invisibility of the tumor on PET (Fig. 6b). There was a significant difference in the uptake of ^{18}F-AlF-NODA-MP-6-Aoc-L5 in the tumor between the inhibition and non-inhibition groups (1.00 ± 0.14%ID/g vs. 2.78 ± 0.42%ID/g, $t = -8.781$, $P = 0.000$) (Fig. 7a). However, no significant difference in the uptake in other organs was noted between these two groups (all $P > 0.05$) (Fig. 7a).

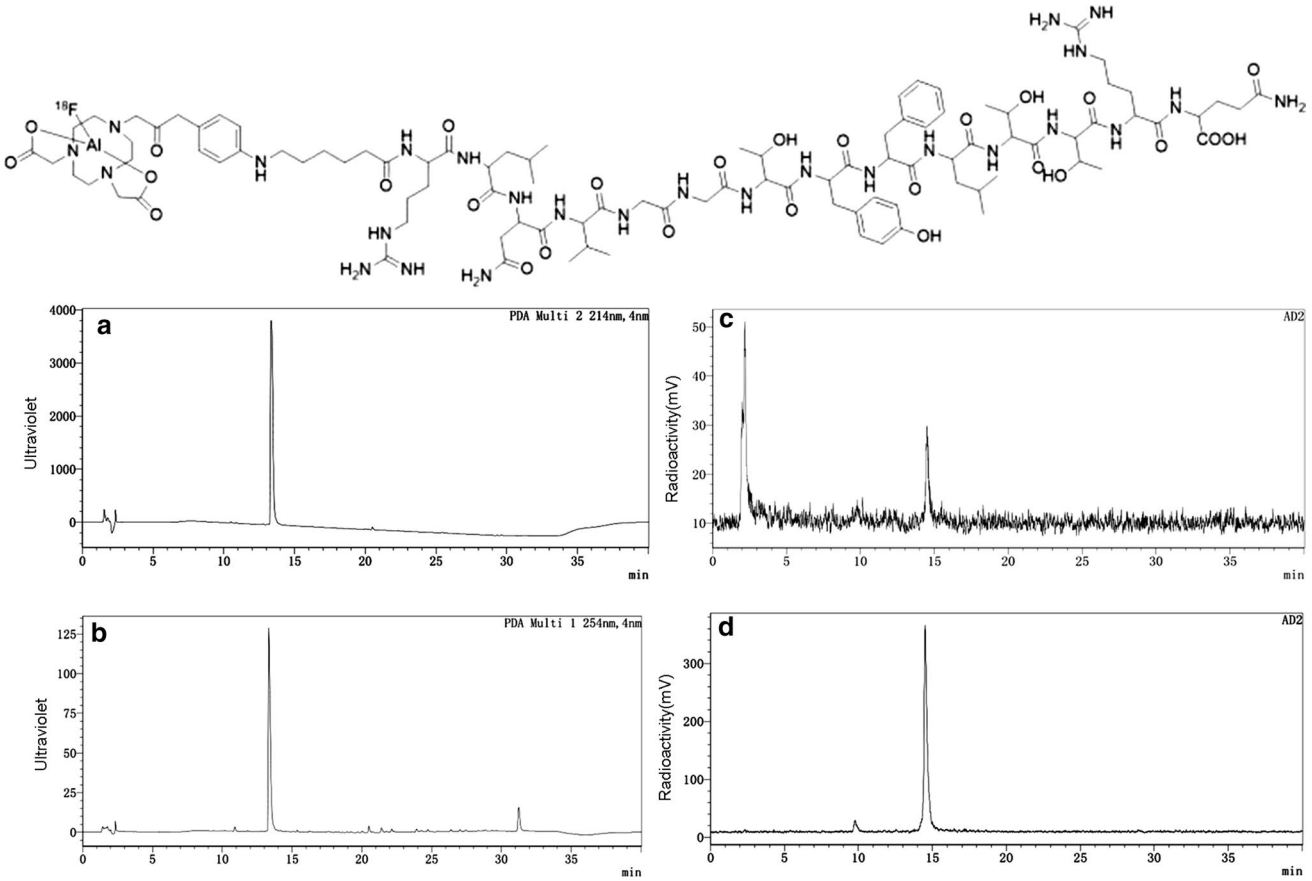

Fig. 4 HPLC analysis for NODA-MP-6-Aoc-L5 and ^{18}F-AlF-NODA-MP-6-Aoc-L5. **a** The HPLC of NODA-MP-6-Aoc-L5 with UV 214 nm, and **b** on UV 254 nm. The retention time was 14.2 min. **c** The HPLC of ^{18}F-AlF-NODA-MP-6-Aoc-L5 before, and **d** after purification. The retention time was 14.7 min. **c** The radiolabeled yield was 29.803%, and **d** the radiochemical purity of the labeled peptides after purification was 95.959%

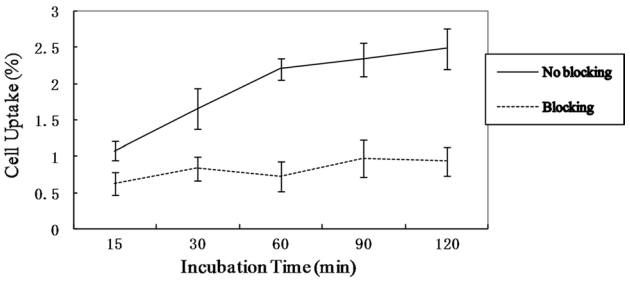

Fig. 5 The cell uptake assay. *Solid line* time-dependent uptake of ^{18}F-AlF-NODA-MP-6-Aoc-L5 in HepG2 cells (n = 3, mean ± SD) without blocking from 15 to 120 min. *Dotted line* time-dependent uptake of ^{18}F-AlF-NODA-MP-6-Aoc-L5 in HepG2 cells (n = 3, mean ± SD) with blocking during the same incubation

Discussion

Because of its potential applicable value, GPC3-targeted imaging has attracted many interests. Although GPC3-specific iron oxide probes have been designed and demonstrated to be able to specifically target GPC3-expressing HepG2 cells in in vitro cellular uptake tests (Park et al. 2011; Li et al. 2012, 2015), no studies have reported the utility of these agents in in vivo MRI imaging. On the other hand, glypican-3-targeted antibody PET imaging has been successfully established. glypican-3-targeted antibody ^{89}Zr PET imaging of hepatocellular carcinoma was reported by Sham et al. (2014a, b) and Yang et al. (2014). In their studies, ^{89}Zr-conjugated mAb could selectively target GPC3 over-expressing HepG2 liver tumors and exhibited high peak uptake of tracers. However, high tumor-to-liver contrast could not be obtained until 3 days after the intravenous injection (Sham et al. 2014b; Yang et al. 2014). To overcome the shortage of long mAb circulation time, ^{89}Zr-conjugated F(ab′)$_2$ fragments directed against GPC3 ^{89}Zr-αGPC3-F(ab′)$_2$) were developed. The blood half-life of the ^{89}Zr-αGPC3-F (ab′) $_2$ conjugate was approximately 11 h, compared with approximately 115 h for the historic mAb controls. This shorter

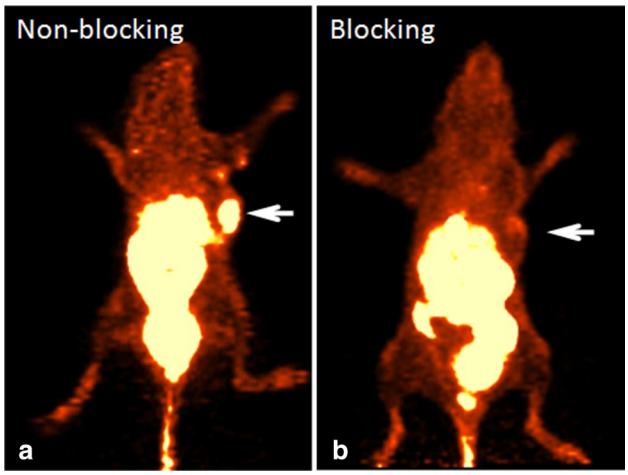

Fig. 6 In vivo detection of HepG2 tumors using ^{18}F-AlF-NODA-MP-6-Aoc-L5 microPET/CT with and without blocking. **a** In vivo micro-PET MIP images of the HepG2 tumor models at 60 min. The tumor (arrow) was visualized clearly. **b** The uptake of ^{18}F-AlF-NODA-MP-C6-L5 in HepG2 tumors was low, and the tumor (arrow) was invisible using PET after inhibition with an excessive quantity of non-conjugated L5 peptide

half-life enabled clear tumor PET visualization 4 h after administration with a high tumor-to-liver contrast ratio (Sham et al. 2014a).

Although the use of ^{89}Zr-conjugated monoclonal antibodies that target GPC3 in PET imaging has shown promise, ^{89}Zr is unavailable in most countries, which limits its wider application. Meanwhile, more radiation exposure is inevitable in subjects undergoing immuno-PET due to the relatively long half-life of ^{89}Zr (Sham et al. 2014a, b; Yang et al. 2014). As an alternative, small molecular ligands, such as peptides, generally possess positive features, such as better clearance kinetics, reasonable metabolic stability and higher tolerance towards bulky modifications. They can also distribute more uniformly and penetrate tissues more readily due to their relatively small size and the fact that they are potentially less immunogenic than proteins because of their lack of a tertiary structure (Wu et al. 2007; Schottelius and Wester 2009). More importantly, they can be labeled with ^{18}F, which can be easily obtained worldwide. Thus, peptides offer the advantage of being both "as large as necessary, and as small as possible" (Wu et al. 2007; Schottelius and Wester 2009; Lee et al. 2011; Wu et al. 2015; Chatalic et al. 2014; Dijkgraaf et al. 2012; McBride et al. 2009; Guo et al. 2012). However, although three GPC3-binding peptide ligands had been successfully identified, L5 (the sequence: RLNVGGTYFLTTRQ) (Lee et al. 2011), TJ12P1 (DHLASLWWGTEL) (Zhu et al. 2016) and GBP (THVSPNQGGLPS) (Qin et al. 2017), glypican-3-targeted peptide PET imaging has not been developed so far.

The present study confirmed that FAM-L5 could be efficiently taken up by GPC3 over-expressed HepG2 cells, but not by GPC3 negatively expressing HL-7702 cells. Confocal fluorescent imaging with a high-powered lens further identified that FAM-L5 accumulated exactly at the site where the GPC3 receptor was located. Meanwhile, the in vitro cell uptake study demonstrated that ^{18}F-AlF-NODA-MP-6-Aoc-L5 can bind to HepG2 tumor cells and was stable in the PBS and mouse serum. These results strengthened the view of Lee et al. (2011) that L5 was a glypican-3-targeting peptide ligand and has the potential to be developed as a novel PET tracer.

The present study also demonstrated that L5 could target GPC3 in vivo. Our study demonstrated that positron emitter (^{18}F) labeled L5 can visualize HepG2 tumors clearly in vivo by microPET/CT scan. The increased uptake of

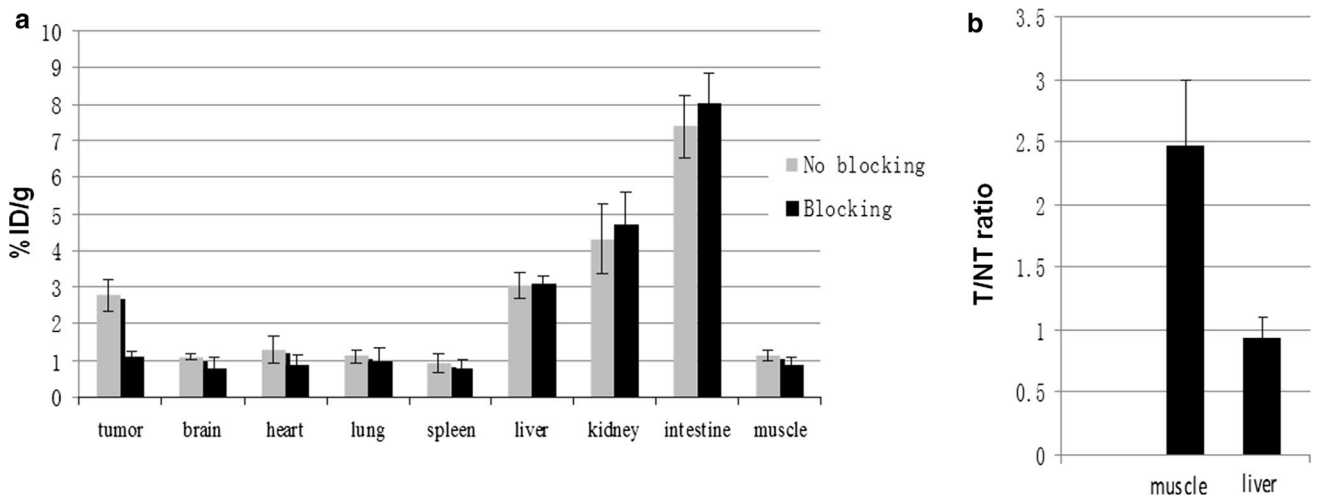

Fig. 7 **a** The in vivo radioactivity biodistribution of ^{18}F-AlF-NODA-MP-6-Aoc-L5 in HepG2 tumor models during inhibition and non-inhibition. **b** The tumor/muscle and tumor/liver ratios

^{18}F-AlF-NODA-MP-6-Aoc-L5 was detected in HepG2 tumors with a medium tumor/muscle ratio (2.46 ± 0.53) at 1 h after injection. The radioactivity was found to be minimal in the brain, head and neck, lungs, heart, muscle and bones, which was useful for lesion detection in these organs. After blocking by excess amounts of non-conjugated L5 peptide, the uptake of the PET tracer was found to dramatically decrease, which indicated that the uptake was receptor specific. However, the present study showed that ^{18}F-AlF-NODA-MP-6-Aoc-L5 presented some deficiency as a PET probe for the detection of liver cancer. Although the addition of the Aoc spacer in the peptide was reported to be useful for increasing excretion in the urinary system and the partition coefficient test suggested that the radiolabeled peptide is rather hydrophilic, the uptake of ^{18}F-AlF-NODA-MP-6-Aoc-L5 in the liver, gallbladder and intestine was still high, which contributed to a low tumor/liver ratio (0.93 ± 0.16) and undesirable radioactivity distribution in the abdomen. To overcome these problems, some modifications should be made in the future, for example, including conjugation of L5 with a more potent hydrophilic linker (GGGRDN) and/or PEG to reduce the excretion of the tracer via the hepatobiliary system and decrease the background radioactivity in the liver and abdomen (Yang et al. 2011; Ma et al. 2012). In addition, in the present study, the affinity of NODA-MP-6-Aoc-L5 seems to be damaged after the addition of an Aoc spacer and modification with NODA. Some alteration is needed to increase the affinity of the tracers in the tumor. Some research studies suggested that designing a dimer L5 may be useful for achieving this aim (Zhang et al. 2006, 2016).

Conclusion

This study demonstrates that FAM-L5 and ^{18}F-AlF-NODA-MP-6-Aoc-L5 can strongly bind HepG2 cells, which showed a high expression of GPC3 receptor. In the subcutaneous xenografts, ^{18}F-AlF-NODA-MP-6-Aoc-L5 can selectively target tumors that highly express GPC-3 and visualize the tumor clearly in vivo with a high tumor/muscle ratio. Therefore, ^{18}F-AlF-NODA-MP-6-Aoc-L5 has a potential to be a PET tracer to document GPC3 receptor expression. However, to become a PET probe for the detection of the tumor in the liver, ^{18}F-AlF-NODA-MP-6-Aoc-L5 needs further chemical modification to achieve a higher tumor/liver ratio.

Acknowledgements We wish to thank our colleagues at the Nanfang PET center and the Department of Oncology and Pathology at the Nanfang Hospital for their support. This work was supported by funding from the National Natural Science Foundation Project of China (81071175, 81371591) and the Natural Science Foundation Project of Guangdong Province (2014A030313311).

Compliance with ethical standards

Conflict of interest The authors declare that they have no conflict of interest.

Informed consent The authors confirm that this work is new and original and not under consideration elsewhere.

Research involving human participants and/or animals This article does not contain any studies with human participants or animals performed by any of the authors.

Financial support National Natural Science Foundation Project of China (81071175, 81371591); Natural Science Foundation Project of Guangdong Province (2014A030313311).

References

Akoad ME, Pomfret EA (2015) Surgical resection and liver transplantation for hepatocellular carcinoma. Clin Liver Dis 19:381–399. https://doi.org/10.1016/j.cld.2015.01.007

Bertino G, Di Carlo I, Ardiri A, Calvagno GS, Demma S, Malaguarnera G, Bertino N, Malaguarnera M, Toro A, Malaguarnera M (2013) Systemic therapies in hepatocellular carcinoma: present and future. Futur Oncol 9:1533–1548. https://doi.org/10.2217/fon.13.171

Bruix J, Sherman M (2011) Management of hepatocellular carcinoma: an update. Hepatology 53:1020–1022. https://doi.org/10.1002/hep.24199

Bruix J, Reig M, Sherman M (2016) Evidence-based diagnosis, staging, and treatment of patients with hepatocellular carcinoma. Gastroenterology 150:835–853. https://doi.org/10.1053/j.gastro.2015.12.041

Chan HL, Hui AY, Wong ML, Tse AM, Hung LC, Wong VW, Sung JJ (2004) Genotype C hepatitis B virus infection is associated with an increased risk of hepatocellular carcinoma. Gut 53:1494–1498. https://doi.org/10.1136/gut.2003.033324

Chan SL, Chan AW, Yeo W (2015) Novel therapeutic targets and predictive markers for hepatocellular carcinoma. Expert Opin Ther Targets 19:973–983. https://doi.org/10.1517/14728222.2015.1031109

Chatalic KL, Franssen GM, van Weerden WM, McBride WJ, Laverman P, de Blois E, Hajjaj B, Brunel L, Goldenberg DM, Fehrentz JA, Martinez J, Boerman OC, de Jong M (2014) Preclinical comparison of Al18F- and 68 Ga-labeled gastrin-releasing peptide receptor antagonists for PET imaging of prostate cancer. J Nucl Med Off Publ Soc Nucl Med 55:2050–2056. https://doi.org/10.2967/jnumed.114.141143

Chen IP, Ariizumi S, Nakano M, Yamamoto M (2014) Positive glypican-3 expression in early hepatocellular carcinoma predicts recurrence after hepatectomy. J Gastroenterol 49:117–125. https://doi.org/10.1007/s00535-013-0793-2

Chen L, Sun J, Yang X (2016) Radiofrequency ablation-combined multimodel therapies for hepatocellular carcinoma: current status. Cancer Lett 370:78–84. https://doi.org/10.1016/j.canlet.2015.09.020

Chuma M, Terashita K, Sakamoto N (2015) New molecularly targeted therapies against advanced hepatocellular carcinoma: from molecular pathogenesis to clinical trials and future directions. Hepatol Res Off J Jpn Soc Hepatol 45:E1–E11. https://doi.org/10.1111/hepr.12459

Coston WM, Loera S, Lau SK, Ishizawa S, Jiang Z, Wu CL, Yen Y, Weiss LM, Chu PG (2008) Distinction of hepatocellular

carcinoma from benign hepatic mimickers using Glypican-3 and CD34 immunohistochemistry. Am J Surg Pathol 32:433–444. https://doi.org/10.1097/PAS.0b013e318158142f

Dijkgraaf I, Franssen GM, McBride WJ, D'Souza CA, Laverman P, Smith CJ, Goldenberg DM, Oyen WJ, Boerman OC (2012) PET of tumors expressing gastrin-releasing peptide receptor with an 18F-labeled bombesin analog. J Nucl Med Off Publ Soc Nucl Med 53:947–952. https://doi.org/10.2967/jnumed.111.100891

Enan ET, El-Hawary AK, El-Tantawy DA, Abu-Hashim MM, Helal NM (2013) Diagnostic role of glypican 3 and CD34 for differentiating hepatocellular carcinoma from nonmalignant hepatocellular lesions. Ann Diagn Pathol 17:490–493. https://doi.org/10.1016/j.anndiagpath.2013.08.001

Feng M, Gao W, Wang R, Chen W, Man YG, Figg WD, Wang XW, Dimitrov DS, Ho M (2013) Therapeutically targeting glypican-3 via a conformation-specific single-domain antibody in hepatocellular carcinoma. Proc Natl Acad Sci USA 110:E1083–E1091. https://doi.org/10.1073/pnas.1217868110

Forner A, Llovet JM, Bruix J (2012) Hepatocellular carcinoma. Lancet 379:1245–1255. https://doi.org/10.1016/S0140-6736(11)61347-0

Gao W, Kim H, Feng M, Phung Y, Xavier CP, Rubin JS, Ho M (2014) Inactivation of Wnt signaling by a human antibody that recognizes the heparan sulfate chains of glypican-3 for liver cancer therapy. Hepatology 60:576–587. https://doi.org/10.1002/hep.26996

Guo N, Lang L, Li W, Kiesewetter DO, Gao H, Niu G, Xie Q, Chen X (2012) Quantitative analysis and comparison study of [18F]AlF-NOTA-PRGD2, [18F]FPPRGD2 and [68 Ga]Ga-NOTA-PRGD2 using a reference tissue model. PLoS One 7:e37506. https://doi.org/10.1371/journal.pone.0037506

Hanaoka H, Nagaya T, Sato K, Nakamura Y, Watanabe R, Harada T, Gao W, Feng M, Phung Y, Kim I, Paik CH, Choyke PL, Ho M, Kobayashi H (2015) Glypican-3 targeted human heavy chain antibody as a drug carrier for hepatocellular carcinoma therapy. Mol Pharm 12:2151–2157. https://doi.org/10.1021/acs.molpharmaceut.5b00132

Ho M, Kim H (2011) Glypican-3: a new target for cancer immunotherapy. Eur J Cancer 47:333–338. https://doi.org/10.1016/j.ejca.2010.10.024

Lai JP, Oseini AM, Moser CD, Yu C, Elsawa SF, Hu C, Nakamura I, Han T, Aderca I, Isomoto H, Garrity-Park MM, Shire AM, Li J, Sanderson SO, Adjei AA, Fernandez-Zapico ME, Roberts LR (2010) The oncogenic effect of sulfatase 2 in human hepatocellular carcinoma is mediated in part by glypican 3-dependent Wnt activation. Hepatology 52:1680–1689. https://doi.org/10.1002/hep.23848

Lee YL, Ahn BC, Lee Y, Lee SW, Cho JY, Lee J (2011) Targeting of hepatocellular carcinoma with glypican-3-targeting peptide ligand. J Pept Sci Off Publ Eur Pept Soc 17:763–769. https://doi.org/10.1002/psc.1400

Li Y, Chen Z, Li F, Wang J, Zhang Z (2012) Preparation and in vitro studies of MRI-specific superparamagnetic iron oxide antiGPC3 probe for hepatocellular carcinoma. Int J Nanomed 7:4593–4611. https://doi.org/10.2147/IJN.S32196

Li YW, Chen ZG, Zhao ZS, Li HL, Wang JC, Zhang ZM (2015) Preparation of magnetic resonance probes using one-pot method for detection of hepatocellular carcinoma. World J Gastroenterol 21:4275–4283. https://doi.org/10.3748/wjg.v21.i14.4275

Libbrecht L, Severi T, Cassiman D, Vander BS, Pirenne J, Nevens F, Verslype C, van Pelt J, Roskams T (2006) Glypican-3 expression distinguishes small hepatocellular carcinomas from cirrhosis, dysplastic nodules, and focal nodular hyperplasia-like nodules. Am J Surg Pathol 30:1405–1411. https://doi.org/10.1097/01.pas.0000213323.97294.9a

Liu H, Li P, Zhai Y, Qu CF, Zhang LJ, Tan YF, Li N, Ding HG (2010) Diagnostic value of glypican-3 in serum and liver for primary hepatocellular carcinoma. World J Gastroenterol 16:4410–4415 **(ISSN:2219-2840 (Electronic); 1007-9327 (Linking))**

Liu X, Wang SK, Zhang K, Zhang H, Pan Q, Liu Z, Pan H, Xue L, Yen Y, Chu PG (2015) Expression of glypican 3 enriches hepatocellular carcinoma development-related genes and associates with carcinogenesis in cirrhotic livers. Carcinogenesis 36:232–242. https://doi.org/10.1093/carcin/bgu245

Ma Y, Yang M, Gao H, Niu G, Yan Y, Lang L, Kiesewetter DO, Chen X (2012) Evaluation of fluorine-labeled gastrin-releasing peptide receptor (GRPR) agonists and antagonists by LC/MS. Amino Acids 43:1625–1632. https://doi.org/10.1007/s00726-012-1238-6

McBride WJ, Sharkey RM, Karacay H, D'Souza CA, Rossi EA, Laverman P, Chang CH, Boerman OC, Goldenberg DM (2009) A novel method of 18F radiolabeling for PET. J Nucl Med Off Publ Soc Nucl Med 50:991–998. https://doi.org/10.2967/jnumed.108.060418

Mittal S, El-Serag HB (2013) Epidemiology of hepatocellular carcinoma: consider the population. J Clin Gastroenterol 47(Suppl):S2–S6. https://doi.org/10.1097/MCG.0b013e3182872f29

Moriguchi M, Umemura A, Itoh Y (2016) Current status and future prospects of chemotherapy for advanced hepatocellular carcinoma. Clin J Gastroenterol 9:184–190. https://doi.org/10.1007/s12328-016-0670-7

Park JO, Stephen Z, Sun C, Veiseh O, Kievit FM, Fang C, Leung M, Mok H, Zhang M (2011) Glypican-3 targeting of liver cancer cells using multifunctional nanoparticles. Mol Imaging 10:69–77 **(ISSN:1536-0121 (Electronic); 1535-3508 (Linking))**

Paul SB, Manjunatha YC, Acharya SK (2009) Palliative treatment in advanced hepatocellular carcinoma: has it made any difference? Trop Gastroenterol 30:125–134 **(ISSN: 0250-636X (Print); 0250-636X (Linking))**

Prasanphanich AF, Nanda PK, Rold TL, Ma L, Lewis MR, Garrison JC, Hoffman TJ, Sieckman GL, Figueroa SD, Smith CJ (2007) [64Cu-NOTA-8-Aoc-BBN(7-14)NH2] targeting vector for positron-emission tomography imaging of gastrin-releasing peptide receptor-expressing tissues. Proc Natl Acad Sci USA 104(30):12462–12467

Prasanphanich AF, Retzloff L, Lane SR, Nanda PK, Sieckman GL, Rold TL, Ma L, Figueroa SD, Sublett SV, Hoffman TJ, Smith CJ (2009) In vitro and in vivo analysis of [64Cu-NO2A-8-Aoc-BBN(7–14)NH2]: a site-directed radiopharmaceutical for positron-emission tomography imaging of T-47D human breast cancer tumors. Nucl Med Biol 36(2):171–181. https://doi.org/10.1016/j.nucmedbio.2008.11.005

Qi XH, Wu D, Cui HX, Ma N, Su J, Wang YT, Jiang YH (2014) Silencing of the glypican-3 gene affects the biological behavior of human hepatocellular carcinoma cells. Mol Med Rep 10:3177–3184. https://doi.org/10.3892/mmr.2014.2600

Qin Z, Wang J, Wang Y, Wang G, Wang X, Zhou Z, Liu G, Gao S, Zhu L (2017) Identification of a glypican-3-binding peptide for in vivo non-invasive human hepatocellular carcinoma detection. Macromol Biosci. https://doi.org/10.1002/mabi.201600335

Samonakis DN, Kouroumalis EA (2017) Systemic treatment for hepatocellular carcinoma: still unmet expectations. World J Hepatol 9:80–90. https://doi.org/10.4254/wjh.v9.i2.80

Sawada Y, Yoshikawa T, Ofuji K, Yoshimura M, Tsuchiya N, Takahashi M, Nobuoka D, Gotohda N, Takahashi S, Kato Y, Konishi M, Kinoshita T, Ikeda M, Nakachi K, Yamazaki N, Mizuno S, Takayama T, Yamao K, Uesaka K, Furuse J, Endo I, Nakatsura T (2016) Phase II study of the GPC3-derived peptide vaccine as an adjuvant therapy for hepatocellular carcinoma patients. Oncoimmunology 5:e1129483. https://doi.org/10.1080/2162402X.2015.1129483

Schottelius M, Wester HJ (2009) Molecular imaging targeting peptide receptors. Methods 48:161–177. https://doi.org/10.1016/j.ymeth.2009.03.012

Sham JG, Kievit FM, Grierson JR, Chiarelli PA, Miyaoka RS, Zhang M, Yeung RS, Minoshima S, Park JO (2014a) Glypican-3-targeting F(ab′)2 for 89Zr PET of hepatocellular carcinoma. J Nucl Med Off Publ Soc Nucl Med 55:2032–2037. https://doi.org/10.2967/jnumed.114.145102

Sham JG, Kievit FM, Grierson JR, Miyaoka RS, Yeh MM, Zhang M, Yeung RS, Minoshima S, Park JO (2014b) Glypican-3-targeted 89Zr PET imaging of hepatocellular carcinoma. J Nucl Med Off Publ Soc Nucl Med 55:799–804. https://doi.org/10.2967/jnumed.113.132118

Shiina S, Tateishi R, Arano T, Uchino K, Enooku K, Nakagawa H, Asaoka Y, Sato T, Masuzaki R, Kondo Y, Goto T, Yoshida H, Omata M, Koike K (2012) Radiofrequency ablation for hepatocellular carcinoma: 10-year outcome and prognostic factors. Am J Gastroenterol 107:569–577. https://doi.org/10.1038/ajg.2011.425 **quiz 578**

Suzuki M, Sugimoto K, Tanaka J, Tameda M, Inagaki Y, Kusagawa S, Nojiri K, Beppu T, Yoneda K, Yamamoto N, Ito M, Yoneda M, Uchida K, Takase K, Shiraki K (2010) Up-regulation of glypican-3 in human hepatocellular carcinoma. Anticancer Res 30:5055–5061 **(ISSN: 1791-7530 (Electronic); 0250-7005 (Linking))**

Torre LA, Bray F, Siegel RL, Ferlay J, Lortet-Tieulent J, Jemal A (2015) Global cancer statistics, 2012. CA Cancer J Clin 65:87–108. https://doi.org/10.3322/caac.21262

Tseng TC, Liu CJ, Yang HC, Su TH, Wang CC, Chen CL, Kuo SF, Liu CH, Chen PJ, Chen DS, Kao JH (2012) High levels of hepatitis B surface antigen increase risk of hepatocellular carcinoma in patients with low HBV load. Gastroenterology 142:1140–1149 e1143. https://doi.org/10.1053/j.gastro.2012.02.007. **(quiz e1113–1144)**

Wu Z, Li ZB, Cai W, He L, Chin FT, Li F, Chen X (2007) 18F-labeled mini-PEG spacered RGD dimer (18F-FPRGD2): synthesis and microPET imaging of alphavbeta3 integrin expression. Eur J Nucl Med Mol Imaging 34:1823–1831. https://doi.org/10.1007/s00259-007-0427-0

Wu HB, Wang Z, Wang QS, Han YJ, Wang M, Zhou WL, Li HS (2015) Use of labelled tLyP-1 as a novel ligand targeting the NRP receptor to image glioma. PLoS One 10:e0137676. https://doi.org/10.1371/journal.pone.0137676

Yan B, Wei JJ, Qian YM, Zhao XL, Zhang WW, Xu AM, Zhang SH (2011) Expression and clinicopathologic significance of glypican 3 in hepatocellular carcinoma. Ann Diagn Pathol 15:162–169. https://doi.org/10.1016/j.anndiagpath.2010.10.004

Yang M, Gao H, Zhou Y, Ma Y, Quan Q, Lang L, Chen K, Niu G, Yan Y, Chen X (2011) F-Labeled GRPR agonists and antagonists: a comparative study in prostate cancer imaging. Theranostics 1:220–229 **(ISSN: 1838-7640 (Electronic); 1838-7640 (Linking))**

Yang X, Liu H, Sun CK, Natarajan A, Hu X, Wang X, Allegretta M, Guttmann RD, Gambhir SS, Chua MS, Cheng Z, So SK (2014) Imaging of hepatocellular carcinoma patient-derived xenografts using (8)(9)Zr-labeled anti-glypican-3 monoclonal antibody. Biomaterials 35:6964–6971. https://doi.org/10.1016/j.biomaterials.2014.04.089

Yao M, Wang L, Dong Z, Qian Q, Shi Y, Yu D, Wang S, Zheng W, Yao D (2014) Glypican-3 as an emerging molecular target for hepatocellular carcinoma gene therapy. Tumour Biol 35:5857–5868. https://doi.org/10.1007/s13277-014-1776-5

Zhang X, Xiong Z, Wu Y, Cai W, Tseng JR, Gambhir SS, Chen X (2006) Quantitative PET imaging of tumor integrin alphavbeta3 expression with 18F-FRGD2. J Nucl Med Off Publ Soc Nucl Med 47:113–121 **(ISSN: 0161-5505 (Print); 0161-5505 (Linking))**

Zhang H, Liu N, Gao S, Hu X, Zhao W, Tao R, Chen Z, Zheng J, Sun X, Xu L, Li W, Yu J, Yuan S (2016) Can an (1)(8)F-ALF-NOTA-PRGD2 PET/CT scan predict treatment sensitivity to concurrent chemoradiotherapy in patients with newly diagnosed glioblastoma? J Nucl Med Off Publ Soc Nucl Med 57:524–529. https://doi.org/10.2967/jnumed.115.165514

Zhu D, Qin Y, Wang J, Zhang L, Zou S, Zhu X, Zhu L (2016) Novel glypican-3-binding peptide for in vivo hepatocellular carcinoma fluorescent imaging. Bioconjug Chem 27:831–839. https://doi.org/10.1021/acs.bioconjchem.6b00030